Desalination and Water Treatment
www.deswater.com

doi: 10.5004/dwt.2022.28855

273 (2022) 114–125
October

Evaluation of changes in activated sludge and sewage sludge quality by FTIR analysis and laser diffraction

Paweł Wiercik[a,*], Magdalena Kuśnierz[a], Małgorzata Kabsch-Korbutowicz[b], Anita Plucińska[a], Przemysław Chrobot[c]

[a]*Institute of Environmental Engineering, Faculty of Environmental Engineering and Geodesy, Wrocław University of Environmental and Life Sciences, Grunwaldzki Square 24, 50–363 Wrocław, Poland, Tel. +48 71 320 10 38; email: pawel.wiercik@upwr.edu.pl (P. Wiercik) ORCID ID: 0000-0001-6093-0611, Tel. +48 71 320 55 72; emails: magdalena.kusnierz@upwr.edu.pl (M. Kuśnierz), anita.plucinska@gmail.com (A. Plucińska)*
[b]*Department of Environment Protection Engineering, Faculty of Environmental Engineering, Wrocław University of Science and Technology, Wybrzeże Wyspiańskiego 27, 50–370 Wrocław, Poland, Tel. +48 71 320 25 02; email: malgorzata.kabsch-korbutowicz@pwr.edu.pl (M. Kabsch-Korbutowicz)*
[c]*Municipal Water and Sewage Company Wrocław, Na Grobli St 14/16, 50–421 Wrocław, Poland, Tel. +48667664509; email: Przemyslaw.Chrobot@mpwik.wroc.pl (P. Chrobot)*

Received 30 December 2021; Accepted 17 August 2022

ABSTRACT

Fourier transform infrared (FTIR) spectroscopy and laser diffraction are commonly applied methods to assess the quality of activated and digested sludge. However, the effect of particle size on FTIR data has never been thoroughly explored. There is also scarce literature on the application of FTIR spectroscopy in conjunction with laser diffraction to investigate changes in the composition and structure of the raw, untreated activated and sewage sludge. In this paper, laser diffraction and FTIR analyses were applied to evaluate the composition, structure and properties of particles in suspensions of activated, thickened and digested sludge samples collected at Janówek Wastewater Treatment Plant (WWTP) located in Wrocław, Poland. FTIR analyses led to the identification of characteristic compounds in the aforementioned types of sludge and processes which they had undergone, for example, decarboxylation and deamination. Laser diffraction tracked the changes in the size and structure of particles in the suspension. Thickened sludge suspensions, which had the largest active surface and the lowest compactness, were characterized by the highest sorption capacity and catalytic activity. The conducted research has shown that the intensity of infrared (IR) absorption is size dependent – smaller particles in the suspension had a higher absorbance intensity in a given wavenumber ranges than larger ones.

Keywords: Fractal dimension; Laser diffraction; Activated sludge; Thickened sludge; Digested sludge; FTIR spectroscopy

1. Introduction

Maintaining optimal operating conditions in microbial processes such as activated sludge or anaerobic digestion is an important aspect of wastewater treatment and waste management. It is necessary to monitor a large number of factors, including physical and morphological properties, chemical compounds, as well as biochemical and biological components of the activated sludge. These factors affect the properties of activated sludge such as compressibility, settleability and dewaterability [1]. Any disruption to this microbial process, which may be manifested as poor settling

* Corresponding author.

of activated sludge, occurrence of unpleasant odor and changes in the appearance and composition of the sludge, decreases the efficiency of sewage treatment. Therefore, the possibility to measure and control activated sludge composition is of crucial importance. Activated sludge is a flocculent suspension composed of microorganisms capable of carrying out the processes of nitrification, denitrification and oxidation of organic compounds. However, bacteria constitute only 5% to 20% of the floc mass, while extracellular polymeric substances (EPS), which are composed of polysaccharides, proteins, lipids and macromolecules and humic substances, account for 50% to 90% of its total organic matter [2,3]. Sewage sludge is a mixture of undigested organics, plant residues, oils or fecal material, inorganic materials, microorganisms and moisture. Undigested organic wastes are a highly heterogeneous mixture of molecules derived from proteins and peptides, lipids, polysaccharides, plant macromolecules with phenolic structures (e.g., lignins or tannins) or aliphatic structures (e.g., cutins or suberins), along with organic micropollutants such as polycyclic aromatic hydrocarbons or dibenzofurans. The inorganic components are mainly the compounds of iron, phosphorus, calcium, aluminum, and sulfur, including traces of heavy metals such as zinc, chromium, mercury, lead, nickel, cadmium and copper [4,5]. During anaerobic digestion, organic materials are broken down by microorganisms into simpler compounds. This process includes the hydrolysis of high-molecular-weight organic compounds and conversion of organic acids (by acid forming bacteria), which occurs simultaneously with gasification of organic acids into methane and carbon dioxide (by acid-splitting methane-forming bacteria) [5,6]. In the course of hydrolysis, suspended organic matter (lipids, proteins, polysaccharides, nucleic acids) is converted into soluble organic monomers (amino acids, long-chain fatty acids). Afterwards, acid-forming bacteria transform the products formed in the hydrolysis stage into short-chain organic acids (volatile fatty acids). In this stage, the formation of acetate, propionate, butyrate, carbon dioxide and hydrogen is observed. In the last stage, methanogens convert acetate and carbon dioxide into methane. Digested sludge contains nutrients (nitrogen, phosphorus) and humic substances and is free from unpleasant odor [7,8].

The properties and behavior of sludge aggregates play a decisive role in the solid–liquid separation processes. The use of FTIR and laser diffraction offers new possibilities in investigating it. FTIR makes it possible to evaluate activated sludge composition and determine its components [9]. It is quick and cost-effective method used to analyze the composition of different media, such as water, soil or plants, by means of capturing spectra of chemicals in the range of IR wavelengths to determine the absorption bands of the substances, thus identify them [9,10]. In the literature there are many publications on using FTIR to examine activated sludge. Some papers focus on EPS from activated sludge and their potential to inhibit the corrosion [11] or adsorb heavy metals [12]; others describe the transformations of sewage sludge when exposed to contaminants [9] or subjected to different disintegration processes [13–15]. However, few publications are devoted to thickened or digested sludge analysis by means of FTIR. Identifying the components of sewage sludge can contribute to assessing its quality, especially in terms of the course and stage of the decomposition processes. To the authors' knowledge, there is also scarce literature on the application of FTIR in conjunction with laser diffraction to investigate changes in the composition and structure of sewage sludge and activated sludge.

Knowledge about the size of particles forming suspensions in water and wastewater is commonly used to select the appropriate water treatment technology and plan the wastewater treatment processes [16]. Nowadays laser diffraction is a commonly accepted method for characterizing activated sludge flocs in terms of size and shape, which may be highly complex and heterogenous. It is known that activated sludge contains relatively small and compact flocs [17].

Changes in the size and structure of activated sludge flocs may indicate, for example, the presence of filamentous bacteria or an increase in organic load. Floc size for a particular shear rate can be a good indicator of floc strength [18]. However, neither fractal dimension nor flocs size are permanent properties, as they change depending on the parameters of the wastewater treatment processes [19].

Laser granulometers are also commonly used to identify the spatial structure of particles based on their fractal dimensions. Fractal dimension D_3 refers to suspension morphology and determines the density ratio of individual particles in a given volume [20]. Both physical and morphological properties affect compressibility, settleability, dewaterability and flocculation of sludge flocs [1,21–23]. Settling and compaction ability of activated sludge are crucial for the overall efficiency of the treatment process and the quality of the receiving water. According to Li et al [23] fractal dimension can be used to predict the settling velocity of flocs; it is correlated with sludge volume index and EPS.

To the authors' knowledge, the simultaneous use of FTIR and particle size distribution (PSD) analyses has rarely been the subject of studies of activated sludge and sewage sludge, as has the analysis of whether IR absorbance is affected by particle size. Moreover, there is little information in the literature about the determination of thickened and digested sludge properties by means of FTIR and laser diffraction; only analyses of the influence of sludge particle size on the intensity of IR absorbance can be found [24,25]. In those studies, however, the authors typically used sewage sludge sieved through a mesh of a particular size, thus obtaining a homogeneous suspension with particles of the same diameter. Results of studies in which the sludge has undergone special treatment, such as drying or sieving, cannot be compared with studies of untreated, highly watered sludge comprising particles of different sizes.

A novel aspect of this study is the simultaneous use of FTIR analysis and particle size analysis to address the question of whether, and to what extent, particle size distribution of suspensions in sediments affects IR absorbance. The study presents the results of FTIR analysis and particle size analysis by means of laser diffraction carried out on activated sludge, thickened sludge and digested sludge samples collected at Janówek WWTP located in Wrocław, Poland, at various stages of their management. The main components of these sludge samples were

identified and changes in the size and spatial structure of the particles forming these sludge suspensions were assessed. An additional aspect of the analyses was to determine whether the particle size of the sludge suspensions influenced the intensity of IR absorbance.

2. Materials and methods

The sludge samples were collected four times (in September, October, November of 2019 and in February of 2020) at Janówek WWTP located in Wrocław, Poland. It is a municipal, mechanical–biological WWTP which treats 140,000 m^3/d of wastewater. The technology line includes: screens, sand separators, primary settling tanks, anaerobic dephosphatation chamber, anoxic denitrification chamber, aerobic nitrification chamber and secondary settling tanks. The primary sludge from primary settling tanks is directed to the gravity sludge thickeners, and subsequently through sludge tank to separate anaerobic digesters. Part of the excess sludge from secondary settling tanks is recirculated to the dephosphatation chamber, and waste activated sludge is directed to the mechanical thickeners, followed by the sludge tank. Both thickened primary sludge and waste activated sludge, are mixed together in the sludge tank, from where they are directed to separate anaerobic digesters. Digested sludge is dewatered on filter presses prior to lime stabilization or drying in the sludge dryer.

Activated sludge was collected directly from the aeration chamber. Thickened and digested sludge samples were collected from the gravity thickener and fermentation chamber, respectively.

The samples were then transported to the Chemical Laboratory of Wrocław University of Environmental and Life Sciences, where attenuated total reflection-Fourier transform infrared (ATR–FTIR) analyses were performed using the Nicolet iN10 integrated infrared microscope with Nicolet iZ10 external FT-IR module (Thermo Fischer Scientific, Waltham, Massachusetts, United States). Each spectrum was the average of 32 scans in the 400–4,000 cm^{-1} wavenumber range at the 4 cm^{-1} spectral resolution. Before FTIR analyses, the sludge samples had to be dewatered (even small amounts of water significantly disrupt the measurements). Since comparable spectra were obtained when dewatering was conducted by means of a vacuum pump, the authors decided to dewater the sludge samples using filters. The dewatering was performed using the Munktell paper disc grade 390 filter placed in a funnel. After 24 h, the sludge sample was subjected to FTIR analysis.

Particle size analysis was conducted in the Geotechnical Laboratory of Wrocław University of Environmental and Life Sciences. PSD and the properties of sewage sludge and activated sludge suspensions were determined with Mastersizer 2000 laser granulometer (Malvern Ltd., Malvern, the United Kingdom) whose particle size measurement range is from 0.02 to 2,000 μm. The granulometer was flushed with water before analysing each sludge sample to remove any possible contaminants from the measuring cell. The flushing was conducted with a stirring speed of 2,500–3,000 rpm. The sludge sample was then poured into a 1 L beaker (which contained water) in an amount sufficient to achieve obscuration range from 10% to 20% (the obscuration level was constantly observed on the monitor screen). The amount of sludge in 800 mL of the solution was about 15–20 mL. Before conducting the analysis, appropriate values of refraction factors for water and sludge had to be entered into the computer (1.33 for water, 1.52 for sludge) and the stirring speed had to be reduced to 1,000 rpm (the lowest speed preventing the sedimentation of suspensions in the beaker). The analysis was performed until subsequent measurements gave similar PSDs. After the measuring cell was flushed again, another sludge sample was analyzed.

The Mastersizer software enables the calculation of the mean diameters and provides the necessary data to determine fractal dimension D_3. The Sauter mean diameter D(3.2), that is, the surface area moment mean diameter, affects the rheological properties of suspensions and provides information about their sorption capacity and catalytic activity (the lower the value of D(3.2), the higher catalytic activity and surface area of particles) [26]. On the other hand, the volume-weighted mean diameter D(4.3) indicates around which central point of the frequency the volume/mass distribution would rotate. Both D(3.2) and D(4.3) are centres of gravity of the respective distributions – surface area or volume/mass [27]. The percentages of particles with given size distributions were also determined. The results are volume- and number-based.

The fractal dimensions of sludge suspensions were calculated by means of an EXCEL spreadsheet provided by the laser granulometer manufacturer. Data obtained from the device, calculated in the spreadsheet, enabled the determination of the fractal dimension D_3. The technique is based on a power law relationship between the total scattering intensity of the light from the aggregates and the magnitude of the scattering vector. By plotting the log of the light scattering intensity as a function of the log of the light scattering vector, the linear slope is the D_3, which varies between 1 and 3 [1].

The values of mean diameters D(3.2), D(4.3), the fractal dimension D_3 and PSDs were analyzed for the effect on IR absorbance intensity in the selected wavenumber ranges.

3. Results and discussion

Fig. 1 shows the ATR-FTIR spectra of the activated sludge samples collected throughout the entire research period. It could be seen, that the activated sludge spectra were characterized by absorption bands at similar wavenumbers. The same tendency was also observed for the thickened and digested sludge samples (Figs. 2 and 3, respectively). The only differences in the shape of the spectra were associated with absorption strength. Changes in the shape of the spectra of activated, thickened and digested sludge collected in September of 2019, as well as the absorption peaks at the specific wavenumbers, are shown in Figs. 4 and 5, respectively. The characteristic IR absorption bands of functional groups detected in the spectra of all sludge samples are summarized in Table 1.

A reduction in absorbance intensity in the region of 1,540 cm^{-1} in digested sludge samples spectra indicated the occurrence of decarboxylation reactions, which result in biogas production with simultaneous release of carbon in the form of CO_2 as well as rapid biodegradation of the

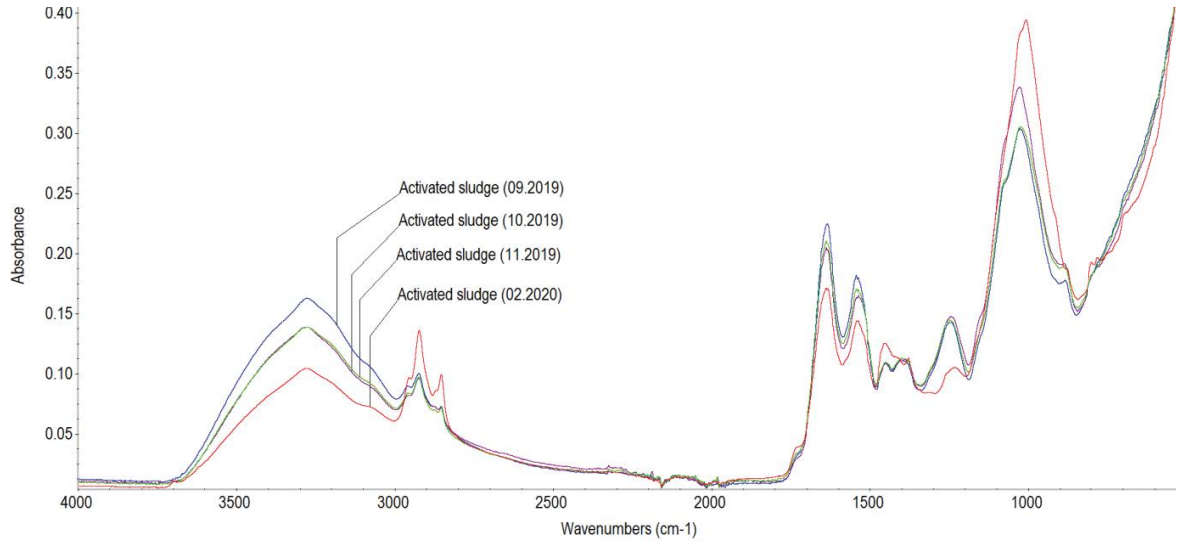

Fig. 1. FTIR spectra of activated sludge samples.

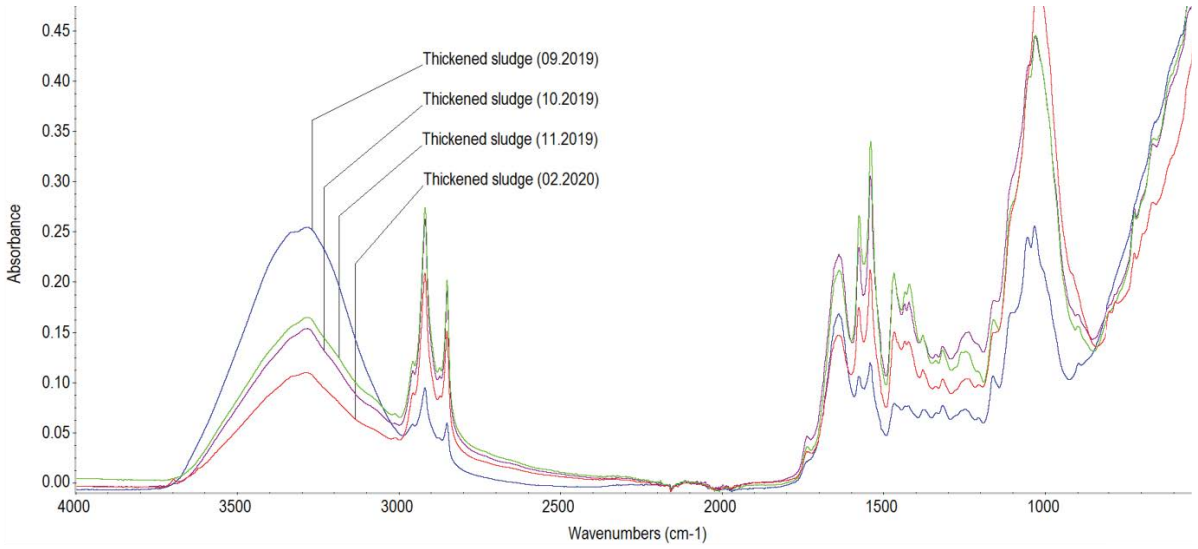

Fig. 2. FTIR spectra of thickened sludge samples.

amino chain [28]. It could also be confirmed by the disappearance of the peak in the digested sludge samples at wavenumber 1,575 cm^{-1}, which was detected in the thickened sludge samples and which indicated the presence of carboxyl groups [29]. According to [30], the C–H groups identified at wavenumbers of 3,000–2,800 and 1,455 cm^{-1} as well as C=O group at wavenumber 1,730 cm^{-1} reflect the occurrence of lipid in digested sludge. At wavenumber 1,410 cm^{-1}, which is a region characteristic for CH_2 in polyalcohols, absorption band could be observed in digested sludge samples. The absorption band at around 1,380 cm^{-1}, which is characteristic for N=O bond in nitrates, occurred in the thickened and digested sludge samples. The presence of nitrates is generally detected in later phases of organics digestion and indicates a state of decomposition in which nitrogen from decomposed components is oxidised [31]. According to Remenárová et al. [32], the functional groups identified at wavenumbers 1,655; 1,535; 1,419 and 1,234 cm^{-1} are characteristic of the bacterial cell wall of both G^+ and G^- bacteria that generally coexist in the activated sludge at biological WWTPs. A peak of 1,231 cm^{-1} was found only in the thickened sludge samples, which may indicate the presence of amides, and thus the decomposition of proteins. In the spectra of thickened sludge samples, absorption peaks at around 1,160 and 1,060 cm^{-1} were observed, which are attributed to C–O–C stretching at the glycosidic linkages and C–O bond stretching vibration in glycerol, respectively. The occurrence of a peak at 1,060 cm^{-1} is an evidence of the presence of fats and fatty acids in the sample [9,31].

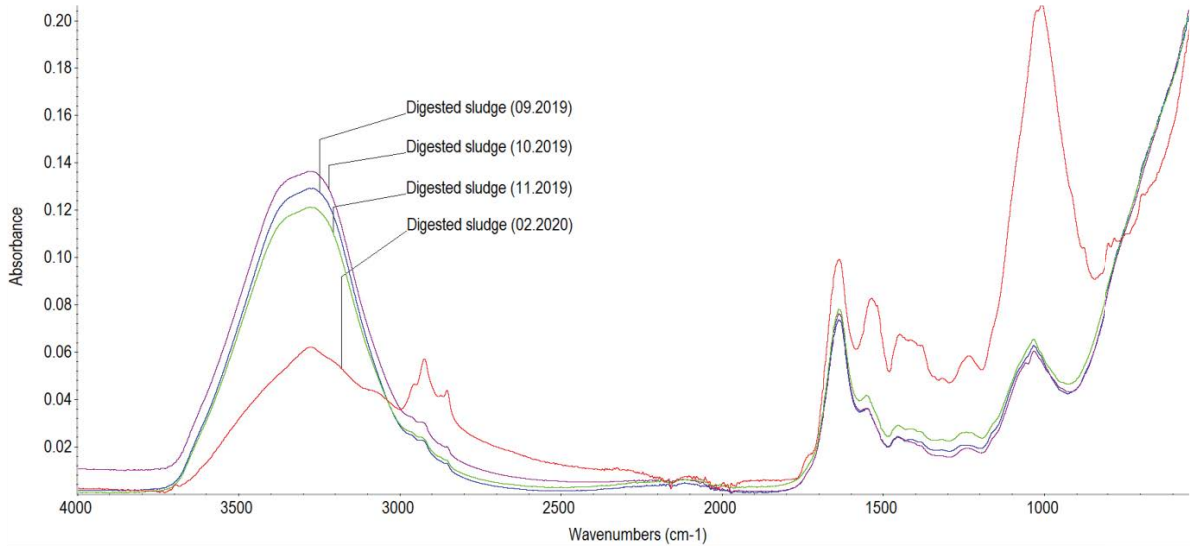

Fig. 3. FTIR spectra of digested sludge samples.

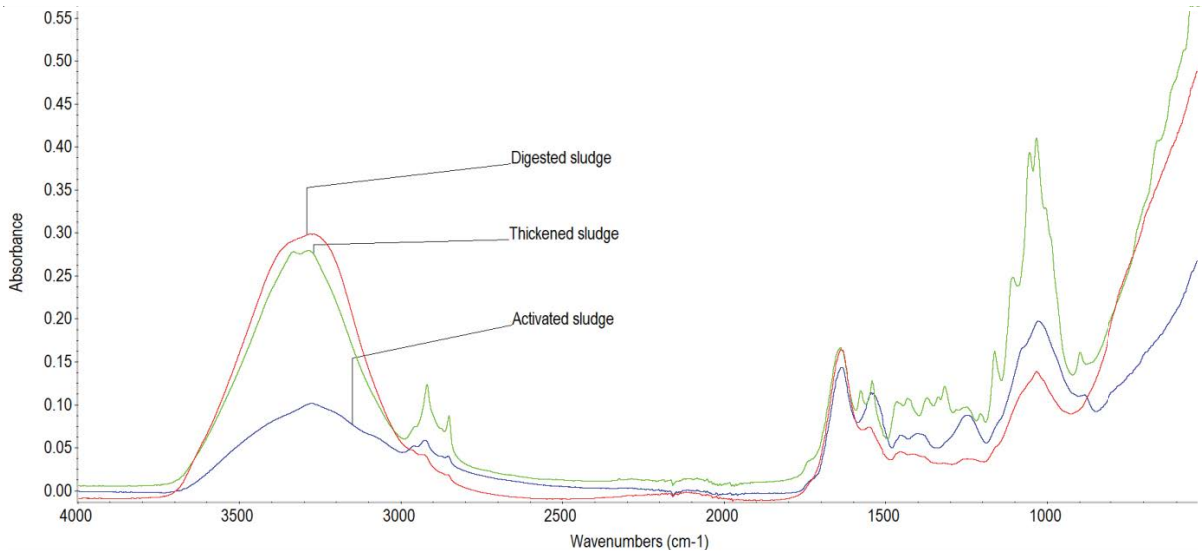

Fig. 4. FTIR spectra of sludge samples collected in September of 2019.

The intensity changes of bands at around 1,030 and 2,930 cm^{-1} in the digested sludge samples (Fig. 3) testified to the occurrence of organic matter decomposition processes [31]. The same tendency was observed in all digested sludge samples collected at Janówek WWTP, but not in the thickened sludge samples, in which only slightly changes at these wavenumbers were observed.

The conducted research demonstrated the usefulness of FTIR to monitor the changes in the composition of activated, thickened and digested sludge. The results indicated the presence of characteristic peaks for polymeric substances, peptides, fats and carboxylic acids. The identified functional groups (O–H, C–N, C=O, N–H, C–H) are typically found in EPS, whereas the identification of bacterial cell walls suggests the presence of microbial organelles. Changes in the intensity of the absorption bands assigned to the aliphatic chains, polysaccharides, carboxylic groups and N–H in proteins indicated, first of all, the presence of lipids, proteins and polysaccharides in digested sludge, and secondly – their biodegradation (decarboxylation, degradation of amino chain). Furthermore, the digested sludge samples spectra exhibited absorption characteristic of the amide groups, pointing to the presence of proteins. The aliphatic chains and C=O groups indicated the presence of humic substances. According to [33], strong aliphaticity and a high nitrogen content in digested sludge may result from the incorporation of proteinaceous materials in humic acids. Réveillé et al. [33] suggest that some lipids remain associated with humic acids by covalent bonds, or are simply trapped in their structure. The conducted FTIR analyses also led to the detection

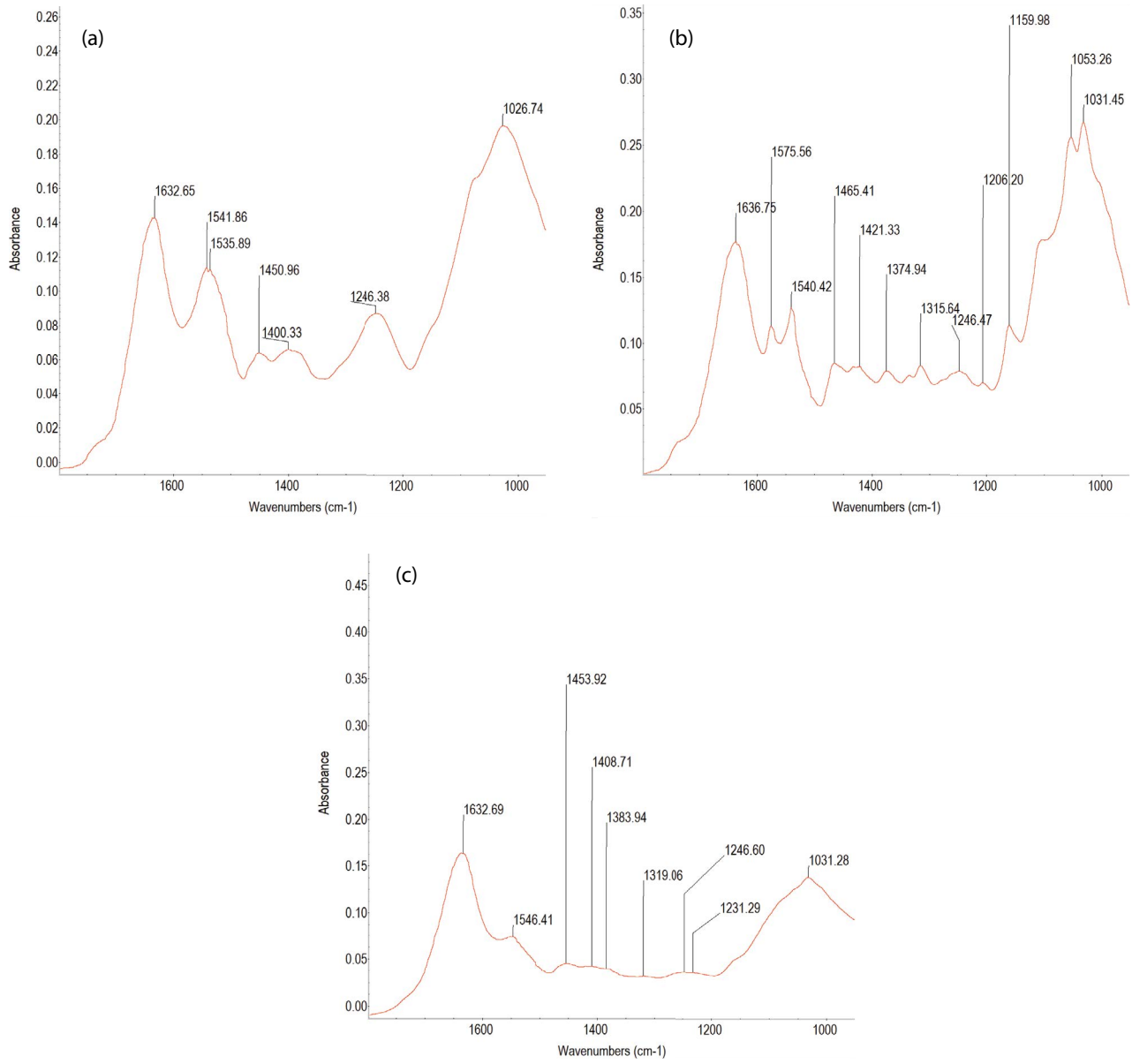

Fig. 5. FTIR spectra of (a) activated sludge, (b) thickened sludge, and (c) digested sludge collected in September 2019.

of lipids and nitrates in digested sludge, and fatty acids in thickened sludge.

Today's approach to the municipal wastewater stream is an approach in the context of water resources, energy and recyclable materials. From this perspective, it is crucial to determine the physicochemical properties of activated sludge and sewage sludge (including functional groups of components), together with the particle size, nano- and microstructures. Research in this field is important, because it can contribute to developing innovative solutions connected with circular economy. There are very few reports on the identity analysis of sludges that differ in terms of PSD.

Subsequent analyses were intended to assess the applicability of laser diffraction in determining the composition and properties of sewage sludge and activated sludge. Figs. 6–8 depict PSD in the total suspended sludge particle volume in activated, thickened and digested sludge samples, respectively. Figs. 9–11 depict PSD in the total suspended sludge particle number in these sludge samples. Fig. 12 shows cumulative graphs, by volume, of all sludge samples collected in subsequent months. It was observed that for activated, thickened and digested sludge samples, PSDs by volume and by number were similar in subsequent series. Unimodal distributions were identified in all samples. The data showed that the particles with a diameter lower than 10 μm and from the range of 20–317 μm accounted for the highest percentage share in PSDs by number and by volume, respectively (Table 2).

Analysis of the data summarized in Table 2 and Figs. 6–11 showed that the particles with the largest volume share in

Table 1
Band assignment in activated sludge (AS), thickened sludge (TS) and digested sludge (DS) samples

Peak position (cm^{-1})	Presence of peak			Literature band value (cm^{-1})	References	Band assignment
	AS	TS	DS			
3330, 3281, 3275	+	+	+	3600–3200	[9,11,14,33]	O–H group in polymeric compounds (polysaccharides, phenols, polyalcohols) and water
				3300–2800	[9,14,30,33]	N–H in amines, proteins, peptides
2950, 2920, 2850	+	+	+	3000–2800	[9,10,30,33]	aliphatic or alicyclic C–H stretching in saccharides, polyalcohols and fats; stretching of aliphatic C–H bond in humic acid
				2925, 2855	[31]	aliphatic methylene groups in fats and lipids
1734	+	+	+	1730, 1720	[9,30,33]	C=O in carboxylic acids and ketonic carbonyls
				1690–1630	[11]	C=O stretch in amide
1636, 1632	+	+	+	1650–1590	[11]	N–H bend in amide (I)
				1634	[14]	C=O groups characteristic for carboxylic acids; C=C in alkenes; O–H group (characteristic for adsorbed water)
1575	–	+	–	1575	[29]	COO– in carboxylic functional groups
				1540–1520	[33]	NH_2 deformation of amide
1546, 1540, 1535	+	+	+	1540	[30]	asymmetric stretching of C=O in carboxylic groups; N–H bending in amide or amino group
				1535	[32]	stretching vibration of C–N and the deformation vibration N–H of the peptidic bond of proteins; bacterial cell wall of both G^+ and G^- bacteria
1465, 1453, 1450	+	+	+	near 1450	[9]	C–H bond vibration in saccharides, N–H group in amides and C–H functional group in alkenes
				1450	[33]	aliphatic C–H deformation
				1440	[9]	CH_2 deformation in fats
				1445–1380	[9]	deforming skeletal vibration of C–H in saccharides
1431, 1421	–	+	+	1419	[32]	vibration of C=O group of carboxylates and carboxylic acids; bacterial cell wall of both G^+ and G^- bacteria
1408	–	–	+	1410	[9]	CH_2 in polyalcohol
1383, 1375	–	+	+	1384, 1380	[9,31]	N=O in nitrates
1246	+	+	+	1245	[9]	deforming vibration of NH^+ in peptides and proteins
				1235,1230	[9,30,32]	vibration of C=O in fats and carboxylic acids
1231	–	+	+	1234	[32]	bacterial cell wall of both G^+ and G^- bacteria
				1230	[30]	C–N stretching of amide II
1160	–	+	–	1160	[31]	C–O–C stretching at the glycosidic linkages
1053	+	+	+	1060	[9]	C–O bond stretching vibration in glycerol (polyalcohol)
				1030	[14,31]	Si–O stretching in the mineral phase of the sludge (silicate impurities and clay minerals possibly in a complex with humic acids);
1031, 1026	+	+	+	1080–1030	[31]	C–O stretching of polysaccharides or polysaccharide-like substances

the total volume of all particles in the suspension were also the least numerous. There were very few largest particles, with diameters above 317 μm, so their quantitative share in all samples was close to 0; however, in the thickened sludge samples, these particles accounted for up to 15% of the total volume of all particles. In the activated sludge samples, the most numerous particles were those with a diameter in the range of 1–20 μm, while in the thickened and digested sludge samples – those with diameters of less than 1 μm (except for the digested sludge sample from November 2019). The volume share of the most numerous particles was negligible and did not exceed several percent. In the activated sludge samples, there were no particles smaller than 1 μm, whose presence could result in the deterioration of the settling processes and dewatering conditions [20].

Discrete data revealed that the size of the smallest particles identified in the activated sludge samples ranged from 2.20 to 2.21 μm, in digested sludge – from 0.55 to 0.6 μm (1.55 to 1.6 μm in November 2019 sample), and in thickened sludge – from 0.35 to 0.65 μm.

Fig. 12 shows PSDs by volume as cumulative frequency curves in subsequent months. As evident, during the digestion process some large flocs were broken up but

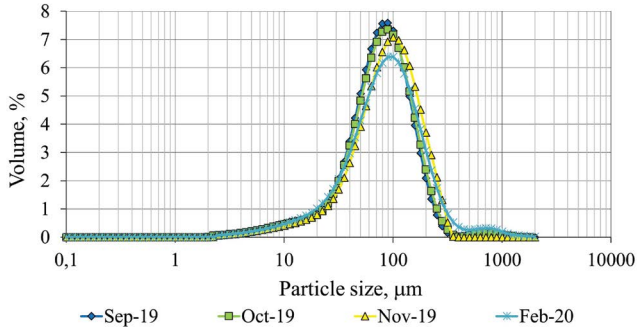

Fig. 6. Percentage share of particles with diameter d_i in the total volume of particles present in activated sludge samples.

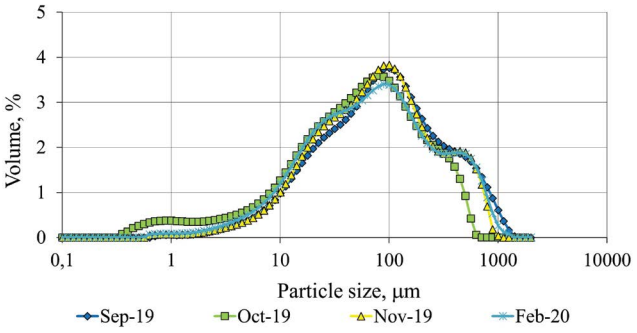

Fig. 7. Percentage share of particles with diameter d_i in the total volume of particles present in thickened sludge samples.

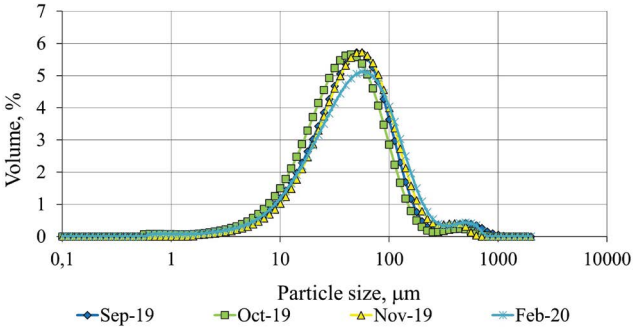

Fig. 8. Percentage share of particles with diameter d_i in the total volume of particles present in digested sludge samples.

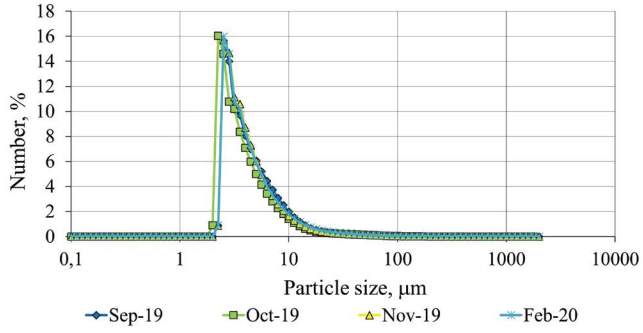

Fig. 9. Percentage share of particles with diameter d_i in the total number of particles present in activated sludge samples.

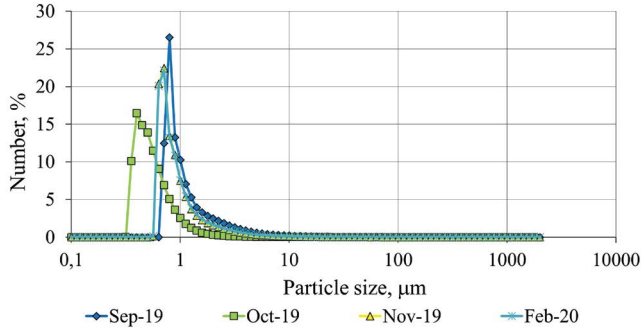

Fig. 10. Percentage share of particles with diameter d_i in the total number of particles present in thickened sludge samples.

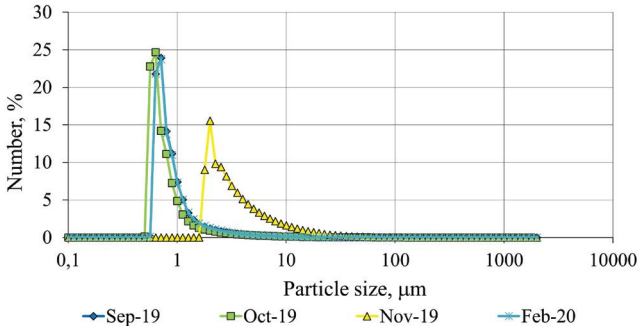

Fig. 11. Percentage share of particles with diameter d_i in the total number of particles present in digested sludge samples.

not destroyed, as the particle volume increased in the small size range. Therefore, the disappearance of large particles represents both the destruction of solids (digestion) and the transfer from large to small particles [34]. In the digested sludge samples around 90% of particles, by volume, had sizes lower than 100 µm. In case of the thickened sludge samples, the share of particles with diameters lower than 100 µm ranged from around 50% to around 65%. Analysis of discrete data in quantitative terms showed that particles in all the samples of thickened and digested sludge were smaller than 100 µm. In the case of the activated sludge samples, only about 0.05% of the particles had diameters greater than 100 µm. Since particles with diameters ranging from 1 to 100 µm have the most significant effect on dewaterability, it can be assumed that digesters at Janówek WWTP ensure not only sludge stabilization, but also its dewaterability [34].

Based on PSDs, the values of mean diameters D(3.2) and D(4.3) and fractal dimension D_3 were determined (Fig. 13). As the D(3.2) diameter decreases, the active surface of particles increases, improving their efficiency in catalyzing chemical processes [20]. The lowest median value of D(3.2) diameters was recorded for suspensions contained in the thickened sludge. The highest values (from 43.06 µm to 48.22 µm) of this mean diameter were observed for the activated sludge samples, which means that the active surface of particles present in the activated sludge suspensions was the lowest; therefore, these particles were characterized by worse sorption capacity and catalytic activity compared

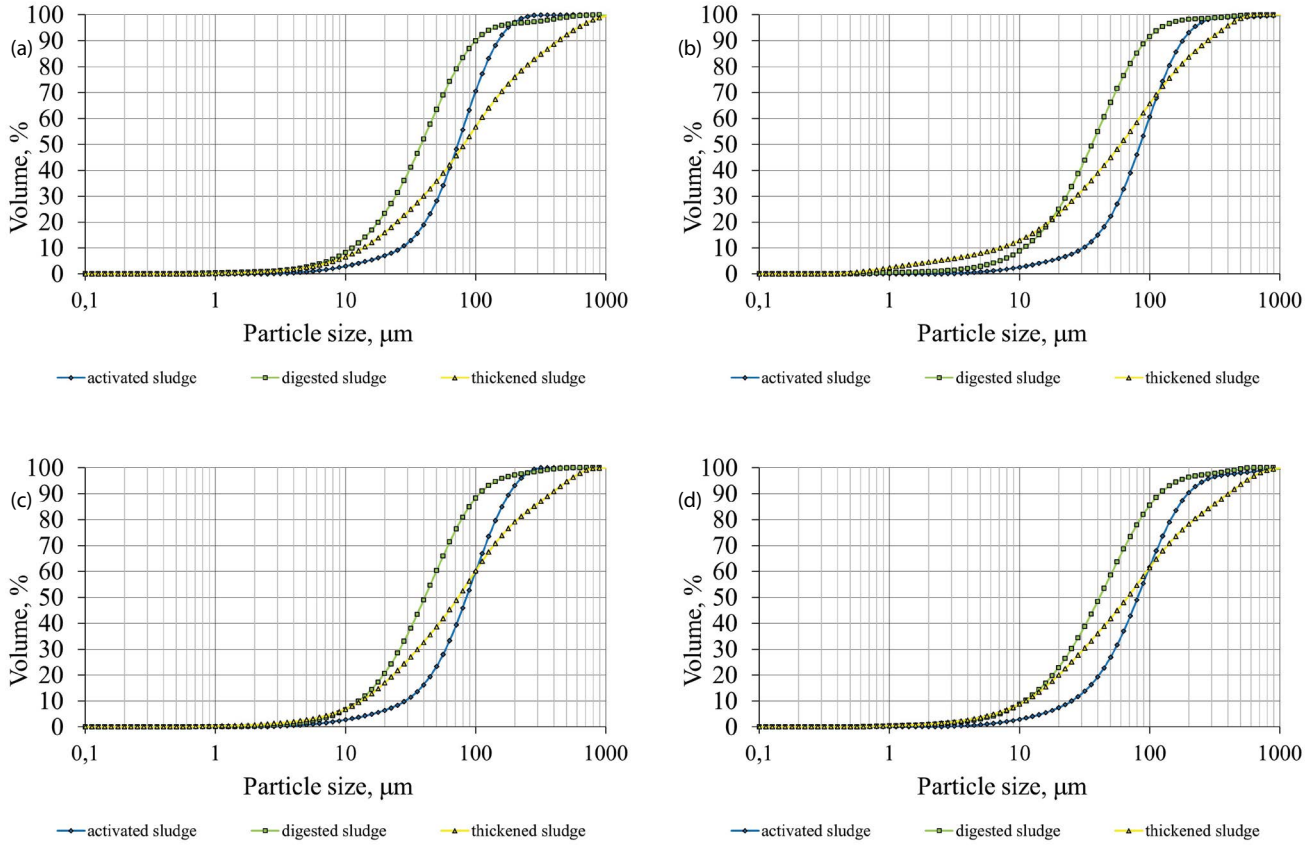

Fig. 12. Cumulative frequency curve of percentage share of particles with diameter d_i in the total volume of particles in all sludge samples collected in: (a) September 2019, (b) October 2019, (c) November 2019, and (d) February 2020.

Table 2
Selected particle size ranges of sludge suspensions by volume and by number

Type of sludge	Size (μm)	PSD by volume (%)	PSD by number (%)
Activated sludge	>317	0.02–3.46	0.00
	20–317	89.14–93.59	2.08–2.50
	1–20	5.96–7.40	97.50–97.92
	<1	0.00	0.00
Digested sludge	>317	1.36–2.72	0.00
	20–317	77.32–81.04	0.13–1.98
	1–20	17.30–20.96	19.97–22.34 (98.02*)
	<1	0.00–0.36	(0.00*) 77.54–79.9
Thickened sludge	>317	7.89–15.21	0.00
	20–317	66.11–70.08	0.01–0.14
	1–20	15.74–20.85	8.69–37.59
	<1	0.19–2.37	62.26–91.30

*percentage share in the sludge sample from November 2019.

to particles in the thickened and digested sludge samples. Despite the concentration of main mass of particles around D(4.3) diameter values of over 10 μm, particles with very small diameters were prevalent in all the sludge samples. This means that a suspension composed of such particles may be classified as poorly sedimenting.

Fractal dimensions of suspensions were determined based on volume PSDs. Such fractal dimensions may take values from 1 to a maximum of 3 [20]. The median of the set of fractal dimension values D_3 for activated sludge was 2.16, for digested sludge – 2.11, and for thickened sludge – 1.88. Suspensions found in the activated and digested sludge samples were characterized by a more cohesive structure than suspensions in the thickened sludge. Activated sludge flocs had the most compact structure (the highest value of fractal dimension) and the smallest specific surface area, which signifies poor ability to adsorb pollutants. These flocs typically have an expanded feathery structure, which explains the higher values of fractal dimensions for these suspensions [20]. Lower values of the fractal dimension of suspensions present in the thickened sludge samples indicated that their spatial structure was more straight, with large open spaces, while the activated and digested sludge samples were characterized by a much higher degree of matter concentration. Flocs with lower values of D_3 contain higher amounts of water, but less bound-water [20]. This means that lower compactness of thickened sludge flocs indicated higher sludge dewaterability, because less water was bound to the solid.

Table 3 summarizes the intensity of IR absorbance in the determined wavenumber ranges in the activated sludge,

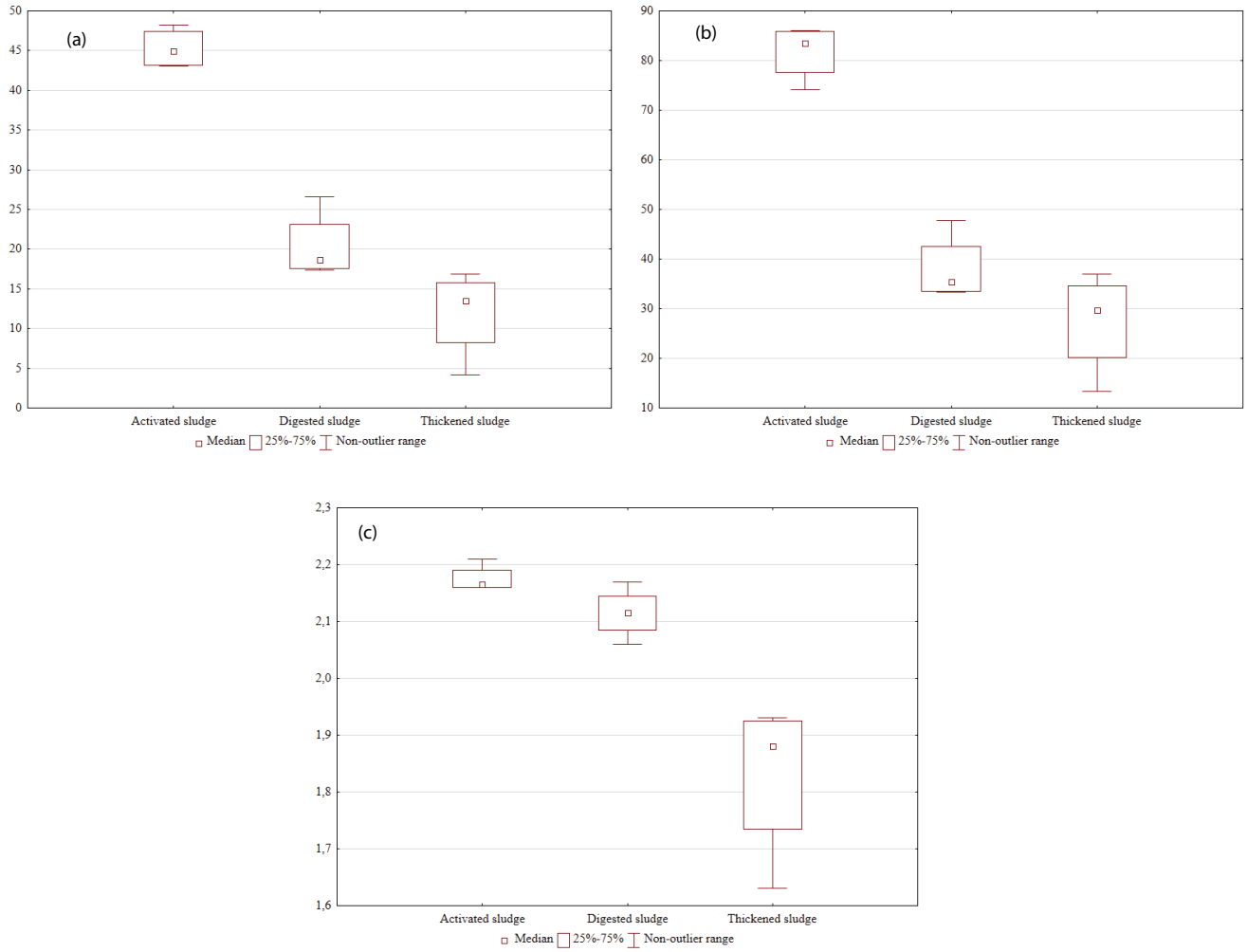

Fig. 13. Comparison of (a) D(3.2) diameter, (b) D(4.3) diameter and (c) fractal dimension values for suspensions in activated, thickened and digested sludge.

Table 3
The intensity of absorption bands in the spectra of activated sludge, digested sludge and thickened sludge

Peak position (cm^{-1})	Activated sludge				Digested sludge				Thickened sludge			
	Date of sample collection											
	09.19	10.19	11.19	02.20	09.19	10.19	11.19	02.20	09.19	10.19	11.19	02.20
	Intensity of absorption bands											
3285–3275	0.10	0.06	0.08	0.08	0.30	0.30	0.29	0.10	0.28	0.15	0.12	0.11
2950–2920	0.06	0.04	0.06	0.06	0.04	0.06	0.05	0.14	0.12	0.24	0.20	0.21
2855–2850	0.04	0.03	0.04	0.04	0.02	0.05	0.02	0.10	0.07	0.18	0.15	0.15
1735	0.01	0.01	0.02	0.02	0.01	0.01	0.02	0.04	0.03	0.05	0.02	0.03
1640–1630	0.14	0.09	0.12	0.13	0.16	0.16	0.19	0.17	0.17	0.21	0.15	0.15
1550–1535	0.11	0.08	0.10	0.11	0.07	0.07	0.09	0.14	0.13	0.28	0.25	0.21
1465–1450	0.06	0.05	0.06	0.07	0.04	0.05	0.06	0.12	0.10	0.19	0.15	0.15
1400–1370	0.07	0.05	0.07	0.07	0.04	0.03	0.06	0.11	0.11	0.14	0.11	0.11
1250–1230	0.09	0.07	0.08	0.09	0.04	0.03	0.05	0.10	0.10	0.14	0.09	0.10
1040–1010	0.20	0.16	0.18	0.22	0.14	0.07	0.15	0.39	0.41	0.40	0.33	0.48

digested sludge and thickened sludge samples to establish if it was size dependent. Analysis of the data from Tables 2 and 3 and Fig. 13 shows that sludge samples with the highest number of the smallest particles (less than 1 μm), the lowest values of diameters D(3.2), D(4.3) and fractal dimension D_3 – that is, the thickened sludge samples – showed the highest IR absorbance values in the entire spectral range. In the activated sludge samples, larger particles (in the range 1–20 μm) were numerically dominant, and the values of diameters D(3.2), D(4.3) and fractal dimension D_3 were the highest. These samples also had the lowest IR absorbance values over the entire spectral range, comparable to absorbance in the digested sludge samples. This means that the smaller particles in the suspensions were characterized by higher intensity of IR absorbance, while larger particles had lower IR absorbance values in the respective wavelength ranges. It corresponds with the results of studies by Udvardi et al. [35], who analyzed monomineralic powders with different particle sizes and showed that as particle size increased, the intensity and area of IR bands usually decreased.

4. Conclusions

The study used FTIR and laser diffraction to investigate the properties of activated, thickened and digested sludge. The conducted research was intended to show whether the quality, structural changes and characteristics of the analyzed sludge samples can be assessed by means of IR spectroscopy and laser diffraction, and whether the absorbance of IR is affected by the particle size. FTIR analysis helped to detect specific functional groups and compounds characteristic for individual sludge sample.

The conducted FTIR analysis of activated, thickened and digested sludge led to the identification of compounds such as polymeric substances, peptides, lipids, humic substances, nitrates and fatty acids, and showed the presence of bacterial cell walls associated with microbial organelles. In addition, compounds found in the analyzed sludge sample provided information about ongoing processes, for example, decarboxylation or deamination.

Laser diffraction supplied information concerning both the properties of particles forming the suspensions and their spatial structure (based on their fractal dimensions). In all the analyzed sludge samples, particles with a diameter of 20–317 μm accounted for the largest part of all particles by volume. However, the most numerous particles were those smaller than 1 μm (in the case of thickened and digested sludge) and 1–20 μm (in activated sludge). Virtually 100% of particles in all the samples had diameters less than 100 μm, which indicated very good dewaterability. Thickened sludge was characterized by the highest dewaterability, as evidenced by the low compactness of flocs, as the content of bound water was lower. On the other hand, the activated sludge samples were characterized by the highest degree of particle density, which resulted from the feathery, complex structure of the flocs. The activated sludge samples also had the worst sorption capacity and catalytic activity. The suspensions of thickened and digested sludge had the largest active surface and the highest sorption capacity and catalytic activity. The conducted research also showed that the intensity of IR absorbance is size dependent. Smaller particles in the suspensions were characterized by a higher absorbance values, whereas particles of larger sizes had lower absorbance values in given wavenumber ranges.

Acknowledgements

This research did not receive any specific grant from funding agencies in the public, commercial, or not-for-profit sectors.

References

[1] B. Jin, B.-M. Wilén, P. Lant, A comprehensive insight into floc characteristics and their impact on compressibility and settleability of activated sludge, Chem. Eng. J., 95 (2003) 221–234.
[2] R. Kocwa-Haluch, T. Woźniakiewicz, Analiza mikroskopowa osadu czynnego i jej rola w kontroli procesu technologicznego oczyszczania ścieków (Microscopic analysis of activated sludge and its role in control of technological process of wastewater treatment), Tech. Trans. Environ. Eng., 108 (2011) 141–162.
[3] M.S. Elliot, Impacts of Operating Parameters on Extracellular Polymeric Substances Production in a High Rate Activated Sludge System Substances Production in a High Rate Activated Sludge System with Low Solids Retention Times, Master's Thesis, Old Dominion University, Norfolk, 2016, doi: 10.25777/5mmx-c139.
[4] V.K. Tyagi, S.-L. Lo, Sludge: a waste or renewable source for energy and resources recovery?, Renewable Sustainable Energy Rev., 25 (2013) 708–728.
[5] A. Demirbas, G. Edris, W.M. Alalayah, Sludge production from municipal wastewater in sewage treatment plant, Energy Sources Part A, 39 (2017) 999–1006.
[6] K. Hagos, J. Zong, D. Li, C. Liu, X. Lu, Anaerobic co-digestion process for biogas production: progress, challenges and perspectives, Renewable Sustainable Energy Rev., 76 (2017) 1485–1496.
[7] L. Appels, J. Baeyens, J. Degrève, R. Dewil, Principles and potential of the anaerobic digestion of waste-activated sludge, Prog. Energy Combust. Sci., 34 (2008) 755–781.
[8] A.M. Anielak, A. Kłeczek, Humus acids in the digested sludge and their properties, Materials, 15 (2022) e1475, doi: 10.3390/ma15041475.
[9] M. Kowalski, K. Kowalska, J. Wiszniowski, J. Turek-Szytow, Qualitative analysis of activated sludge using FT-IR technique, Chem. Pap., 72 (2018) 2699–2706.
[10] P. Wiercik, B. Frączek, P. Chrobot, Fouling of anion exchanger by image and FTIR analyses, J. Environ. Chem. Eng., 8 (2020) e103761, doi: 10.1016/j.jece.2020.103761.
[11] L.C. Go, W. Holmes, D. Depan, R. Hernandez, Evaluation of extracellular polymeric substances extracted from waste activated sludge as a renewable corrosion inhibitor, Peer J., 7 (2019) e7193, doi: 10.7717/peerj.7193.
[12] Y. Liu, W. Lv, Z. Zhang, S. Xia, Influencing characteristics of short-time aerobic digestion on spatial distribution and adsorption capacity of extracellular polymeric substances in waste activated sludge, RSC. Adv., 8 (2018) 32172–32177.
[13] T. Liu, Y. Guo, N. Peng, Q. Lang, Y. Xia, C. Gai, Z. Liu, Nitrogen transformation among char, tar and gas during pyrolysis of sewage sludge and corresponding hydrochar, J. Anal. Appl. Pyrolysis, 126 (2017) 298–306.
[14] E. Feki, A. Battimelli, S. Sayadi, A. Dhouib, S. Khoufi, High-rate anaerobic digestion of waste activated sludge by integration of electro-Fenton process, Molecules, 25 (2020) e626, doi: 10.3390/molecules25030626.
[15] S. Yildiz, A. Cömert, Fenton process effect on sludge disintegration, Int. J. Environ. Health Res., 30 (2020) 89–104.

[16] P. Wiercik, K. Matras, E. Burszta-Adamiak, M. Kuśnierz, Analysis of the properties and particle size distribution of spent filter backwash water from groundwater treatment at various stages of filter washing, Eng. Prot. Environ., 19 (2016) 149–161.
[17] M. Kuśnierz, Scale of small particle population in activated sludge flocs, Water Air Soil Pollut., 229 (2018) e327, doi: 10.1007/s11270-018-3979-7.
[18] W. Burger, K. Krysiak-Baltyn, P.J. Scales, G.J. Martin, A.D. Stickland, S.L. Gras, The influence of protruding filamentous bacteria on floc stability and solid–liquid separation in the activated sludge process, Water Res, 123 (2017) 578–585.
[19] M. Xie, C. Wang, X. Liu, R. Xiong, Y. Xu, Characteristics of biochemical and fractal structure of activated sludge with thermochemical lysis, Water Air Soil Pollut., 228 (2017) e187, doi: 10.1007/s11270-017-3351-3.
[20] M. Kuśnierz, P. Wiercik, Analysis of particle size and fractal dimensions of suspensions contained in raw sewage, treated sewage and activated sludge, Arch. Environ. Prot., 42 (2016) 67–76.
[21] Y. Fan, X. Ma, X. Dong, Z. Feng, Y. Dong, Characterisation of floc size, effective density and sedimentation under various flocculation mechanisms, Water Sci. Technol., 82 (2020) 1261–1271.
[22] Z. Li, P. Lu, D. Zhang, F. Song, Simulation of floc size distribution in flocculation of activated sludge using population balance model with modified expressions for the aggregation and breakage, Math. Probl. Eng., 2019 (2019) 5243860, doi: 10.1155/2019/5243860.
[23] Z.-H. Li, Y. Guo, Z.-Y. Hang, T. Zhang, H.-Q. Yu, Simultaneous evaluation of bioactivity and settleability of activated sludge using fractal dimension as an intermediate variable, Water Res., 178 (2020) e115834, doi: 10.1016/j.watres.2020.115834.
[24] Q. Dai, X. Jiang, G. Lv, X. Ma, Y. Jin, F. Wang, Y. Chi, J. Yan, Investigation into particle size influence on PAH formation during dry sewage sludge pyrolysis: TG-FTIR analysis and batch scale research, J. Anal. Appl. Pyrolysis, 112 (2015) 388–393.
[25] L. Yan, Y. Liu, Y. Wen, Y. Ren, G. Hao, Y. Zhang, Role and significance of extracellular polymeric substances from granular sludge for simultaneous removal of organic matter and ammonia nitrogen, Bioresour. Technol., 179 (2015) 460–466.
[26] D.L. Black, M.Q. McQuay, M.P. Bonin, Laser-based techniques for particle-size measurement: a review of sizing methods and their industrial applications, Prog. Energy Combust., 22 (1996) 267–306.
[27] Malvern Instruments Ltd., Basic Principles of Particle Size Analysis. Available at: https://www.atascientific.com.au/wp-content/uploads/2017/02/AN020710-Basic-Principles-Particle-Size-Analysis.pdf, (Accessed 14 December 2021).
[28] P.J. Arauzo, M. Atienza-Martínez, J. Ábrego, M.P. Olszewski, Z. Cao, A. Kruse, Combustion characteristics of hydrochar and pyrochar derived from digested sewage sludge, Energies, 13 (2020) e4164, doi: 10.3390/en13164164.
[29] J.L. Masengo, J. Mulopo, Synthesis and performance evaluation of adsorbents derived from sewage sludge blended with waste coal for nitrate and methyl red removal, Sci. Rep., 12 (2022) 1–22.
[30] J.-P. Cao, L.-Y. Li, K. Morishita, X.-B. Xiao, X.-Y. Zhao, X.-Y. Wei, T. Takarada, Nitrogen transformations during fast pyrolysis of sewage sludge, Fuel, 104 (2013) 1–6.
[31] M. Grube, J.G. Lin, P.H. Lee, S. Kokorevicha, Evaluation of sewage sludge-based compost by FT-IR spectroscopy, Geoderma, 130 (2006) 324–333.
[32] L. Remenárová, M. Pipíška, M. Horník, M. Rozložník, J. Augustín, J. Lesný, Biosorption of cadmium and zinc by activated sludge from single and binary solutions: mechanism, equilibrium and experimental design study, J. Taiwan Inst. Chem. Eng., 43 (2012) 433–443.
[33] V. Réveillé, L. Mansuy, É. Jardé, É. Garnier-Sillam, Characterisation of sewage sludge-derived organic matter: lipids and humic acids, Org. Geochem., 34 (2003) 615–627.
[34] D.F. Lawler, Y.J. Chung, S.-J. Hwang, B.A. Hull, Anaerobic digestion: effects on particle size and dewaterability, J. Water Pollut. Control Fed., 58 (1986) 1107–1117.
[35] B. Udvardi, I.J. Kovács, T. Fancsik, P. Kónya, M. Bátori, F. Stercel, G. Falus, Z. Szalai, Effects of particle size on the attenuated total reflection spectrum of minerals, Appl. Spectrosc., 71 (2017) 1157–1168.